Physica A 462 (2016) 38–47

Contents lists available at ScienceDirect

Physica A

journal homepage: www.elsevier.com/locate/physa

A sliding mode controller for vehicular traffic flow

Yongfu Li [a,b,*], Yuhao Kang [a], Bin Yang [a], Srinivas Peeta [b,c], Li Zhang [a], Taixong Zheng [a], Yinguo Li [a]

[a] Center for Automotive Electronics and Embedded System, College of Automation, Chongqing University of Posts and Telecommunications, Chongqing 400065, China

[b] NEXTRANS Center, Purdue University, West Lafayette, IN 47906, USA

[c] School of Civil Engineering, Purdue University, West Lafayette, IN 47907, USA

HIGHLIGHTS

- A sliding model controller is proposed for vehicular traffic flow.
- The stability of the controller is guaranteed using the Lyapunove technique.
- Numerical experiments are performed to compare the performance of SMC with that of feedback control.
- Results illustrate the effectiveness of the proposed SMC method in terms of smoothness and stability.

ARTICLE INFO

Article history:
Received 27 April 2016
Received in revised form 23 May 2016
Available online 17 June 2016

Keywords:
Car-following model
Traffic flow
Sliding mode control
Feedback control
Lyapunov technique

ABSTRACT

This study proposes a sliding mode controller for vehicular traffic flow based on a car-following model to enhance the smoothness and stability of traffic flow evolution. In particular, the full velocity difference (FVD) model is used to capture the characteristics of vehicular traffic flow. The proposed sliding mode controller is designed in terms of the error between the desired space headway and the actual space headway. The stability of the controller is guaranteed using the Lyapunov technique. Numerical experiments are used to compare the performance of sliding mode control (SMC) with that of feedback control. The results illustrate the effectiveness of the proposed SMC method in terms of the distribution smoothness and stability of the space headway, velocity, and acceleration profiles. They further illustrate that the SMC strategy is superior to that of the feedback control strategy, while enabling computational efficiency that can aid in practical applications.

1. Introduction

Over the past few decades, there has been a lot of focus on capturing the complex mechanisms behind the phenomena of vehicular traffic flow from the microscopic and macroscopic viewpoints. Consequently, various traffic flow models such as cellular automaton (CA) models, car-following (CF) models, lattice hydrodynamic models, and gas kinetic models [1,2] have been proposed. In this context, the optimal velocity (OV) based CF models have been in focus recently to address two important aspects. The first is the descriptive traffic flow modeling, which addresses the underlying mechanisms behind the traffic flow phenomena. The second is the normative traffic flow control, which focuses on congestion mitigation and the smoothness of traffic flow evolution.

* Corresponding author at: Center for Automotive Electronics and Embedded System, College of Automation, Chongqing University of Posts and Telecommunications, Chongqing 400065, China.
E-mail address: laf1212@163.com (Y. Li).

http://dx.doi.org/10.1016/j.physa.2016.06.053
0378-4371/

From the traffic flow modeling perspective, the CF models can be classified as lane-discipline and non-lane-discipline based models. The lane-discipline-based CF models assume that vehicles follow the lane discipline and move in the middle of the lane without lateral gaps. Bando et al. [3] propose the OV model based on the assumption that the following vehicle seeks a safe velocity determined by the space headway from the leading vehicle. Thereafter, various variations of OV-based CF models have been developed by factoring the surroundings of the following vehicle [4–21], such as generalized force (GF) mode [4], full velocity difference (FVD) model [5], multiple ahead and velocity difference (MAVD) model [6], full velocity and acceleration difference (FVAD) model [7], multiple velocity difference (MVD) model [8], and multiple headway, velocity and acceleration difference (MHVAD) model [9]. Results from these CF models show that the stop-and-go waves can be captured effectively. Unlike the lane-discipline-based CF models, the non-lane-discipline-based CF models allow for the scenario that lanes may not be clearly demarcated on a road though multiple vehicles can travel in parallel, or that lane-discipline may not be respected. Jin et al. [22] propose a non-lane-based full velocity difference CF (NLBCF) model to analyze the impact of the lateral gap on one side of the CF behavior. However, the NLBCF model cannot distinguish the right-side or the left-side lateral gaps. Consequently, Li et al. [23] propose a generalized model which considers the effects of two-sided lateral gaps of the following vehicle under the non-lane-discipline environment. Li et al. [24] further study the effects of lateral gaps on the energy consumption for electric vehicle flow under the non-lane discipline. The aforementioned studies also illustrate that CF models can effectively capture the characteristics of traffic flow phenomena in the real world.

From the traffic flow control perspective, control can be used to mitigate traffic congestion or seek the smooth flow of traffic. Konishi et al. [25] simplify the stability condition of OV model under the periodic boundary situation. Konishi et al. [26] propose a decentralized delayed-feedback control mechanism to address traffic congestion based on the OV model. Zhao et al. [27] propose a feedback control approach to reduce traffic jams based on the OV model, where the velocity difference between the leading and following vehicle is designed as the feedback signal. Li et al. [28] propose an acceleration feedback control strategy for traffic jam suppression based on the FVD model. Li et al. [29] propose a delay feedback control strategy of vehicular traffic flow based on the lattice model by considering the difference of the density change rate. The aforementioned studies analyze vehicular traffic flow control using the feedback control strategy. However, the computational time required for enabling smoothness and stability of the space headways and velocities of vehicular traffic flow using such feedback control strategies needs to be reduced given the real-time needs of traffic control. This represents the motivation for the current study which develops a new computationally efficient sliding mode control (SMC) strategy to improve the traffic flow evolution smoothness and stability.

This study focuses on designing a computationally efficient sliding mode controller of vehicular traffic flow based on the FVD model efficiently so as to enable the traffic flow to be smooth and stable. The FVD model is used to capture the characteristics of vehicular traffic flow. The sliding mode controller is designed in terms of the error between the desired space headway and the actual space headway between the leading and following vehicles. The stability of the controller is guaranteed using the Lyapunov technique. Simulation-based numerical experiments are used to compare the performance of the proposed SMC strategy with that of a feedback control strategy. The results indicate that the SMC strategy performs better than the feedback control strategy, in terms of the distribution smoothness and stability associated with the space headway, velocity, and acceleration profiles.

The rest of this paper is organized as follows. Section 2 reviews the FVD model used to model traffic flow in this study. Section 3 designs the sliding mode controller using the Lyapunov technique. Section 4 discusses the numerical experiments to compare traffic profiles with respect to the space headway, velocity, and acceleration profiles. The final section provides some concluding comments.

2. FVD model

As shown in Fig. 1, for the lane-discipline-based scenario in car-following theory, Jiang et al. [5] propose the FVD model to capture the characteristics of vehicular traffic flow by considering both the positive and negative velocity differences between the leading and following vehicles:

$$a_i(t) = k[V(y_i(t)) - v_i(t)] + \lambda \Delta v_i(t), \tag{1}$$

where $x_i(t)$, $v_i(t)$ and $a_i(t)$ represent the position (in m), velocity (in m/s) and acceleration (in m/s^2), respectively, of vehicle i at time t. $y_i(t) \equiv x_{i+1}(t) - x_i(t)$ and $\Delta v_i(t) \equiv v_{i+1}(t) - v_i(t)$ are the space headway difference and velocity difference between the leading vehicle $i+1$ and the following vehicle i. $k > 0$ ($k \in \mathbb{R}$) and $\lambda \geq 0$ ($\lambda \in \mathbb{R}$) are the sensitivity coefficients.

$V(y_i(t))$ is the optimal velocity function [5]:

$$V(y_i(t)) = [\tanh(y_i(t) - x_c) + \tanh(c_c)]v_{\max}/2 \tag{2}$$

where $v_{\max}$ is the maximal speed of the vehicle, x_c is the safe space headway, and $\tanh(\bullet)$ is the hyperbolic tangent function.

Eq. (1) can be rewritten as:

$$\frac{\mathrm{d}^2 x_i(t)}{\mathrm{d}t^2} = k\left[V(y_i(t)) - \frac{\mathrm{d}x_i(t)}{\mathrm{d}t}\right] + \lambda \Delta v_i(t). \tag{3}$$

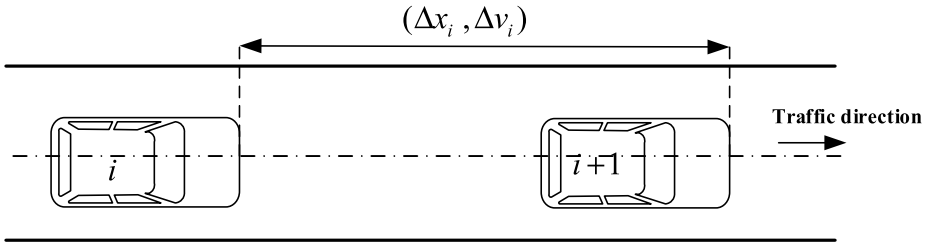

Fig. 1. Lane-discipline-based car-following model.

Based on the discussion heretofore, the FVD model can be rewritten as:

$$\begin{cases} \dfrac{\mathrm{d}^2 x_i(t)}{\mathrm{d}t^2} = k\left[V(y_i(t)) - \dfrac{\mathrm{d}x_i(t)}{\mathrm{d}t}\right] + \lambda \Delta v_i(t) \\ y_i(t) = \Delta x_i(t) = x_{i+1}(t) - x_i(t) \\ \Delta v_i(t) = v_{i+1}(t) - v_i(t) \end{cases} \quad (i = 1, \ldots, N). \tag{4}$$

Further,

$$\begin{cases} \dfrac{\mathrm{d}v_i(t)}{\mathrm{d}t} = k[V(y_i(t)) - v_i(t)] + \lambda(v_{i+1}(t) - v_i(t)) \\ \dfrac{\mathrm{d}y_i(t)}{\mathrm{d}t} = v_{i+1}(t) - v_i(t) \end{cases} \quad (i = 1, \ldots, N). \tag{5}$$

Let the vehicular traffic flow occur with the desired (optimal) constant velocity v_0 under steady state conditions. The corresponding space headway between the leading and following vehicles is $V^{-1}(v_0)$ based on Eq. (2). The steady state of the following vehicle is [26–28]:

$$[v_i^*(t), y_i^*(t)]^{\mathrm{T}} = [v_0, V^{-1}(v_0)]^{\mathrm{T}}. \tag{6}$$

Therefore, Eq. (5) can be linearized in the neighborhood of the steady state as shown in Eq. (6). Then, we obtain:

$$\begin{cases} \dfrac{\mathrm{d}\delta v_i(t)}{\mathrm{d}t} = k[\Lambda \delta y_i(t) - \delta v_i(t)] + \lambda(\delta v_{i+1}(t) - \delta v_i(t)) \\ \dfrac{\mathrm{d}\delta y_i(t)}{\mathrm{d}t} = \delta v_{i+1}(t) - \delta v_i(t) \end{cases} \quad (i = 1, \ldots, N) \tag{7}$$

where $\delta v_i(t) = v_i(t) - v_0$, $\delta y_i(t) = y_i(t) - V^{-1}(v_0)$, and Λ is as follows:

$$\Lambda = \left.\frac{\mathrm{d}V(y_i(t))}{\mathrm{d}y_i(t)}\right|_{y_i(t)=V^{-1}(v_0)}. \tag{8}$$

Define $\delta v_i(t)$ and $\delta y_i(t)$ as the system state variables. The state-space representation of the vehicular traffic system can be obtained as:

$$\begin{bmatrix} \dfrac{\mathrm{d}\delta v_i(t)}{\mathrm{d}t} \\ \dfrac{\mathrm{d}\delta y_i(t)}{\mathrm{d}t} \end{bmatrix} l = \begin{bmatrix} -k-\lambda & k\Lambda \\ -1 & 0 \end{bmatrix} \begin{bmatrix} \delta v_i(t) \\ \delta y_i(t) \end{bmatrix} + \begin{bmatrix} \lambda \\ 1 \end{bmatrix} \delta v_{i+1}(t). \tag{9}$$

Following the approach proposed by Konishi et al. [26], we add a control signal term $u_i(t)$ to Eq. (9), and obtain:

$$\begin{bmatrix} \dfrac{\mathrm{d}\delta v_i(t)}{\mathrm{d}t} \\ \dfrac{\mathrm{d}\delta y_i(t)}{\mathrm{d}t} \end{bmatrix} = \begin{bmatrix} -k-\lambda & k\Lambda \\ -1 & 0 \end{bmatrix} \begin{bmatrix} \delta v_i(t) \\ \delta y_i(t) \end{bmatrix} l + \begin{bmatrix} \lambda \\ 1 \end{bmatrix} \delta v_{i+1}(t) + \begin{bmatrix} 1 \\ 0 \end{bmatrix} u_i(t). \tag{10}$$

According to Ref. [7], λ can be chosen as:

$$\lambda = \begin{cases} 0.5\ \mathrm{s}^{-1}, & y_i(t) \le 100 \\ 0, & y_i(t) > 100. \end{cases} \tag{11}$$

3. Controller design

We first specify a feedback control strategy that is used to compare with the SMC strategy proposed in this paper. Then, the SMC strategy is described.

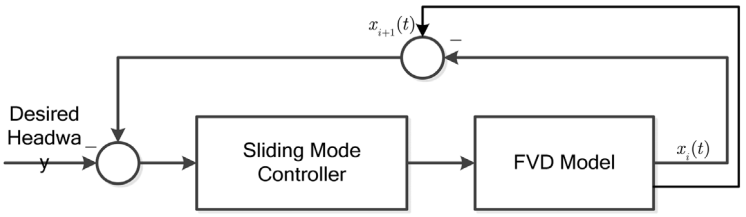

Fig. 2. Control scheme.

3.1. Feedback control law

The feedback control strategy based on the FVD model is as follows [28]:

$$u_i(t) = k\left[\frac{\mathrm{d}v_{i+1}(t-1)}{\mathrm{d}t} - \frac{\mathrm{d}v_i(t-1)}{\mathrm{d}t}\right] \tag{12}$$

where k is now labeled the adjustable feedback gain in the control strategy.

3.2. SMC law

To improve the control performance in terms of the smoothness and stability, we design a sliding model controller of the vehicular traffic system. Fig. 2 illustrates the FVD model based SMC strategy for the vehicular traffic system.

To begin with, as shown in Fig. 2, we suppose $V^{-1}(v_0)$ is the desired space headway, and the error between the actual space headway and desired space headway is defined as follows:

$$s_0 = \delta y_i(t) = y_i(t) - V^{-1}(v_0). \tag{13}$$

Therefore, the goal of SMC is $\lim_{t\to\tau} s_0 = 0$, where τ represents a finite time constant, and $\tau > 0$.

Based on the SMC theory, the sliding mode surface is defined as follows [30–32]:

$$s = s_0 + c_1\dot{s}_0, \tag{14}$$

where $c_1 \in \mathbb{R}$ and $c_1 > 0$.

Using Lyapunov-based control design methods, a sliding mode controller for the vehicular traffic system can be designed as follows:

$$u_i(t) = \frac{1}{c_1}\left\{[c_1(k+\lambda)-1]\delta v_i(t) - c_1 k\Lambda\delta y_i(t) - c_1\lambda\delta v_{i+1}(t) + \delta v_{i+1}(t) + c_1\frac{\mathrm{d}\delta v_{i+1}(t)}{\mathrm{d}t} + \eta s + \varphi\,\mathrm{sgn}(s)\right\}, \tag{15}$$

where $\eta \in \mathbb{R}$ and $\eta > 0$, $\varphi \in \mathbb{R}$ and $\varphi > 0$.

3.3. Stability analysis

To facilitate the stability analysis of designed sliding mode controller, we choose the candidate Lyapunov function as follows:

$$E = \frac{1}{2}s^2. \tag{16}$$

Since,

$$\begin{aligned}
\dot{s} &= \dot{s}_0 + c_1\ddot{s}_0 \\
&= \delta v_{i+1}(t) - \delta v_i(t) + c_1\left[-\frac{\mathrm{d}\delta v_i(t)}{\mathrm{d}t} + \frac{\mathrm{d}\delta v_{i+1}(t)}{\mathrm{d}t}\right] \\
&= \delta v_{i+1}(t) - \delta v_i(t) + c_1\left[(k+\lambda)\delta v_i(t) - k\Lambda\delta y_i(t) - \lambda\delta v_{i+1}(t) - u_i(t) + \frac{\mathrm{d}\delta v_{i+1}(t)}{\mathrm{d}t}\right] \\
&= [c_1(k+\lambda)-1]\delta v_i(t) - c_1 k\Lambda\delta y_i(t) - c_1\lambda\delta v_{i+1}(t) - c_1 u_i(t) + \delta v_{i+1}(t) + c_1\frac{\mathrm{d}\delta v_{i+1}(t)}{\mathrm{d}t}.
\end{aligned} \tag{17}$$

Then, we have:

$$\begin{aligned}
\dot{E} &= s\dot{s} \\
&= s\left\{[c_1(k+\lambda)-1]\delta v_i(t) - c_1 k\Lambda\delta y_i(t) - c_1\lambda\delta v_{i+1}(t) - c_1 u_i(t) + \delta v_{i+1}(t) + c_1\frac{\mathrm{d}\delta v_{i+1}(t)}{\mathrm{d}t}\right\}.
\end{aligned} \tag{18}$$

Substituting Eq. (15) into Eq. (18), and noting that $\eta > 0$ and $\varphi > 0$, we obtain:

$$\dot{E} = s\dot{s} = s(-\eta s - \varphi \operatorname{sgn}(s)) = -\eta s^2 - \varphi |s| \leq 0. \tag{19}$$

Hence, based on the Lyapunov stability theory, we know that the proposed controller is stable.

Theorem 1. *With the proposed controller in (15), if the control system is Lyapunov stable, then we can simultaneously obtain:*

$$\lim_{t\to\infty} s(t) = 0, \qquad \lim_{t\to\infty} s_0(t) = 0, \qquad \lim_{t\to\infty} \dot{s}_0(t) = 0. \tag{20}$$

Proof. According to Eq. (19), since $\dot{E} \leq 0$, we know that E is a non-increasing function when $t \in [0, \infty)$. So, $E(t) \leq E(0) < \infty$.

Since,

$$\ddot{E} = -2\eta s\dot{s} - \varphi \dot{s} |s| . \tag{21}$$

Based on Eqs. (13) and (14), we know that $s_0(t)$ and $s(t)$ are bounded when $t \geq 0$. Since $\dot{s}_0 = \dot{y}_i(t)$, we know that $\dot{s}_0 \in \mathcal{L}_\infty$. Furthermore, from (21), we know that $\dot{E}$ is uniformly continuous because $\ddot{E} \in \mathcal{L}_\infty$.

In addition, we have:

$$\int_0^\infty \left|\dot{E}\right| \mathrm{d}t = |E(\infty)| - |E(0)| < \infty. \tag{22}$$

From Eq. (22), we know that $\dot{E} \in \mathcal{L}_2$. Hence, $\lim_{t\to\infty} \dot{E} = 0$ based on Barbalat's Lemma [31–33]. Moreover, we know $\dot{E} = s(-\eta s - \varphi \operatorname{sgn}(s)) \leq 0$. Thus, we have $\lim_{t\to\infty}(\eta s^2 + \varphi |s|) = 0$. Consequently, we have $\lim_{t\to\infty} s(t) = 0$, $\lim_{t\to\infty} s_0(t) = 0$, $\lim_{t\to\infty} \dot{s}_0(t) = 0$. □

Therefore, the sliding mode tends to converge toward the surface $s = 0$ in finite time when the control system is Lyapunov stable [34–36].

4. Numerical experiments

In order to verify the effectiveness of the proposed sliding model controller, we perform simulation-based numerical experiments. Consider a road of length L. Let there be N vehicles running on a single lane under an open boundary. The related parameters are set as:

$$x_c = 2.0\ \mathrm{m}, \qquad v_{\max} = 2\ \mathrm{m/s}, \qquad v_0 = 0.94\ \mathrm{m/s}, \qquad \lambda = 0.5, \qquad N = 100, \qquad L = 200\ \mathrm{m}.$$

We use the Runge–Kutta algorithm for numerical integration with time-step $\Delta t = 0.01$ s. The uniform random noise with maximum amplitude 10^{-3} is added to the first equation of (4) for all vehicles. The initial conditions are chosen as $\Delta x_i(0) = x_c$, $(i = 2, \ldots, N)$, $x_i(0) = V^{-1}(x_c) = v_0$. For analysis, two cases are considered in terms of the control strategy for the vehicular traffic flow. The first has no control strategy, and the second compares the SMC and feedback control strategies.

Case I: Without control strategy

The spatio-temporal pattern of the vehicular traffic flow induced by the noise in the FVD model without control after $t = 100$ s is shown in Fig. 3. It exhibits phase segregation into unsmooth region upstream and smooth region downstream. Figs. 4 and 5 show the variations of space headway and velocity profiles of vehicular traffic flow at $t = 100$ s and $t = 500$ s, respectively. Fig. 4 indicates that the space headway oscillates around the constant headway x_c upstream at $t = 100$ s, and gradually becomes constant downstream at $t = 500$ s. Fig. 5 illustrates that the velocity of the upstream vehicular traffic flow oscillates around the constant velocity v_0 at $t = 100$ s, and the downstream vehicular traffic flow travels with a constant velocity v_0 at $t = 500$ s. Also, the oscillation amplitude converges toward to constant with the increase of the car index. The plots in the figures suggest that vehicular traffic flow fluctuations occur in the noisy FVD model without control strategy.

Case II: With control strategy

In this section, the performance of the SMC is compared with that of the feedback control for vehicular traffic flow. Initially, based on the designed sliding mode controller as shown in Eq. (15), the parameters of the proposed controller are chosen as:

$$c_1 = 2.3, \qquad k = 0.1, \qquad \eta = 1, \qquad \varphi = 1.$$

Figs. 6 and 7 illustrate the spatio-temporal patterns of vehicular traffic flow from 70 s to 100 s under the feedback control and sliding mode control strategies, respectively. By comparing with Fig. 3, it can be noted the traffic flow fluctuation can be stabilized effectively using control strategies. In addition, from Figs. 6 and 7, it also shows that the SMC strategy in Fig. 7 performs better than the feedback control strategy with respect to the spatio-temporal pattern of the vehicular traffic flow since the ripple occurs in Fig. 6.

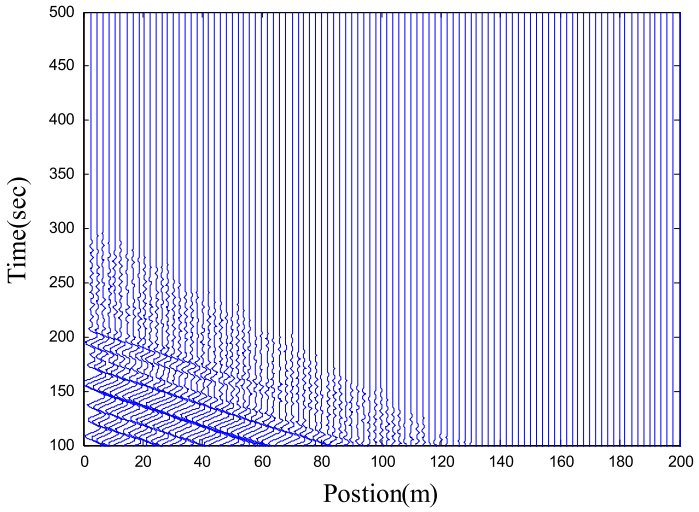

Fig. 3. Spatio-temporal pattern of vehicular traffic flow without control ($t = 100$–500 s).

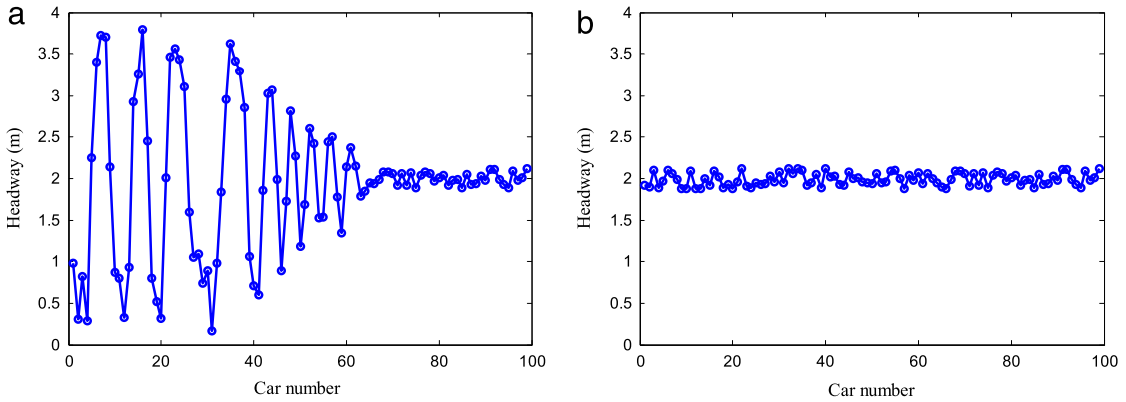

Fig. 4. Space headway profile of vehicular traffic flow without control strategy: (a) $t = 100$ s; (b) $t = 500$ s.

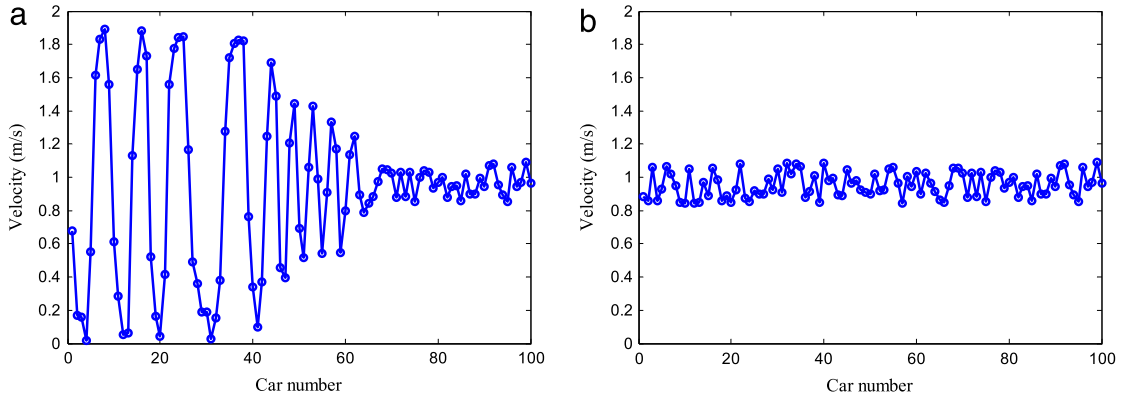

Fig. 5. Velocity profile of vehicular traffic flow without control strategy: (a) $t = 100$ s; (b) $t = 500$ s.

Figs. 8 and 10 illustrate the space headway profiles of vehicular traffic flow at $t = 50$ s and $t = 100$ s, respectively. Similarly, Figs. 9 and 11 illustrate the velocity profiles of vehicular traffic flow at $t = 50$ s and $t = 100$ s, respectively. Figs. 8(a) and 10(a) are the space headway profiles and Figs. 9(a) and 11(a) are velocity profiles under the feedback control strategy. Figs. 8(b) and 10(b) are the space headway profiles and Figs. 9(b) and 11(b) are velocity profiles under the SMC strategy. Comparing Figs. 8(a) and (b), it can be observed that the space headway profile of vehicular traffic flow under the feedback control strategy fluctuates around the constant space headway at $t = 50$ s, with a range between 1.5 and 2.5 m.

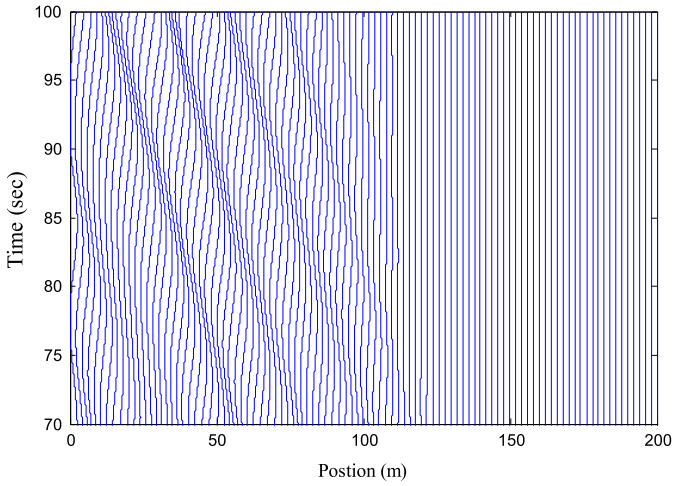

Fig. 6. Spatio-temporal pattern of vehicular traffic flow under the feedback control strategy ($t = 70$–100 s).

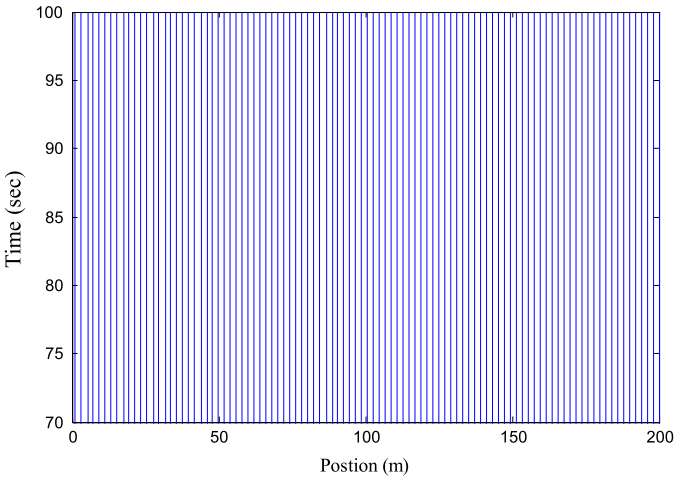

Fig. 7. Spatio-temporal pattern of vehicular traffic flow under the SMC strategy ($t = 70$–100 s).

By contrast, the space headway profile of vehicular traffic flow under the SMC strategy is much smoother. Figs. 9(a) and (b) indicate that the velocity profile of vehicular traffic flow under the feedback control strategy fluctuates around the constant velocity at $t = 50$ s, with a range between 0.6 and 1.4 m/s. In comparison, the velocity profile of vehicular traffic flow under the SMC strategy is much smoother.

From Figs. 10(a), (b), 11(a) and (b), it can be observed that when the time approaches 100 s, both the space headway and velocity profiles of vehicular traffic flow under the feedback control and SMC strategies are in a relatively stable state. Based on the discussion heretofore, the vehicular traffic flow under the SMC strategy converges to the steady state more quickly compared with those under the feedback control strategy and no control strategy. This implies that the smoothness and stability of the traffic flow evolution associated with the space headway and velocity is improved through the use of the SMC strategy.

The acceleration (or deceleration) of vehicles is the underlying factor that causes a variation in the vehicular traffic flow state. To verify this aspect, Fig. 12 shows the acceleration profile of vehicular traffic flow under the feedback control and SMC strategies at $t = 400$ s. From Fig. 12(a) and (b), the fluctuation of acceleration of vehicular traffic flow under the SMC strategy is much smaller than that under the feedback control strategy. It indicates that the SMC strategy has a positive impact on the traffic flow evolution compared with the feedback control strategy. It also implies that SMC strategy can improve the stability and smoothness of vehicular traffic flow effectively.

In summary, by comparing the numerical experiment results of the no control, feedback control and SMC strategies, the following key findings can be identified:

(i) Compared with a no control strategy, the use of a control strategy for vehicular traffic flow can enhance the distribution smoothness associated with the spatio-temporal pattern, and space headway and velocity profiles.

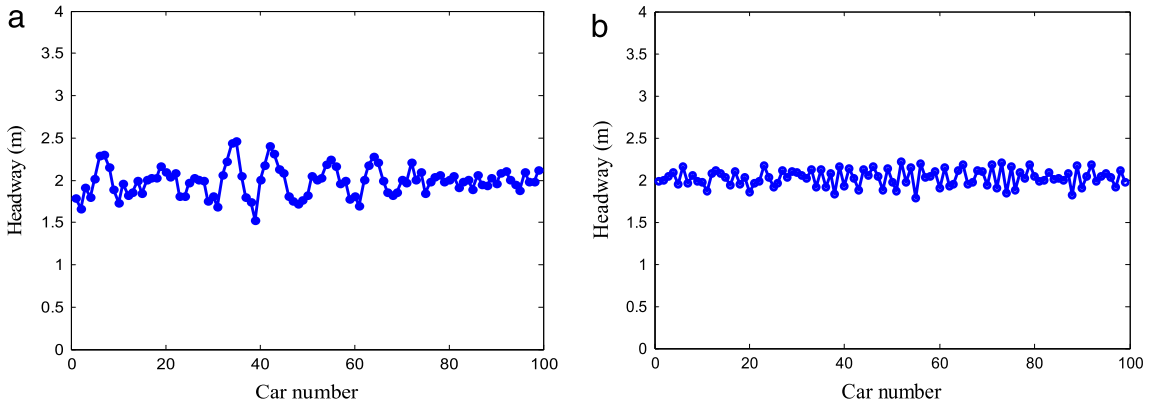

Fig. 8. Space headway profile of vehicular traffic flow ($t = 50$ s): (a) Feedback control strategy; (b) SMC strategy.

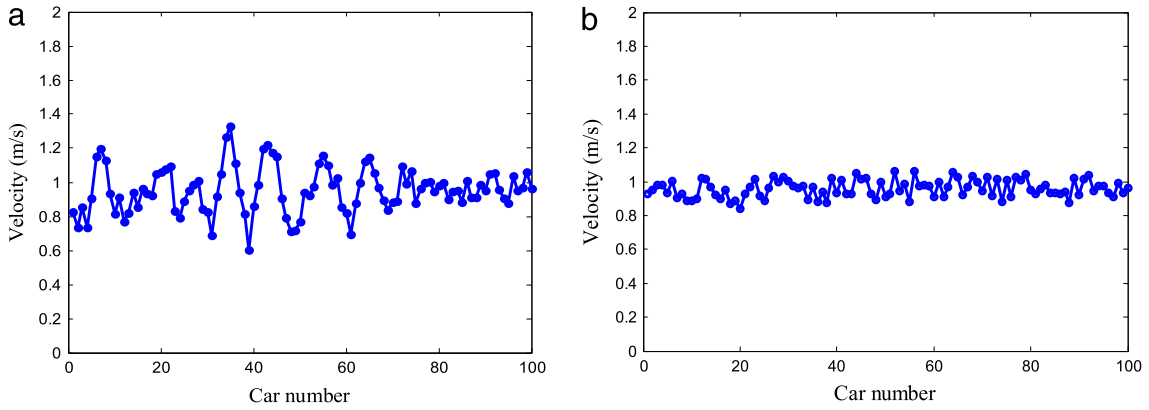

Fig. 9. Velocity profile of vehicular traffic flow ($t = 50$ s): (a) Feedback control strategy; (b) SMC strategy.

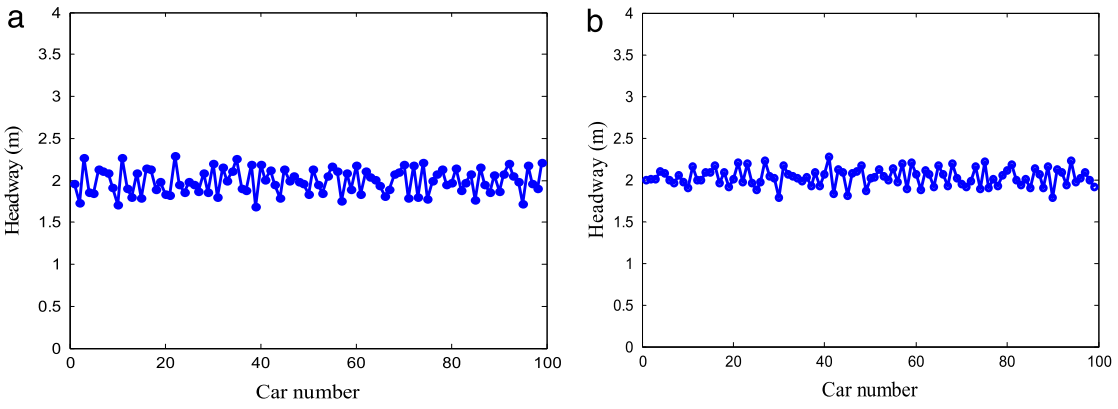

Fig. 10. Space headway profile of vehicular traffic flow ($t = 100$ s): (a) Feedback control strategy; (b) SMC strategy.

(ii) The SMC strategy performs better than the feedback control strategy in terms of the smoothness and stability of the space headway and velocity profiles of vehicular traffic flow. In particular, the proposed SMC strategy can lead to smoothness and stability more quickly than the feedback control strategy. This has implications in a deployment context, given the computational time constraints associated with enabling real-time control in practical applications.

(iii) Fig. 12 verifies that the acceleration profile of vehicular traffic flow is a key underlying factor that affects the variation of traffic flow state over time.

(iv) The traffic flow profiles, including the space headway, velocity and acceleration of vehicular traffic flow in Figs. 3–12, indicate that disturbances or effects always propagate from downstream to upstream, that is, in the direction opposite to the movement of vehicles.

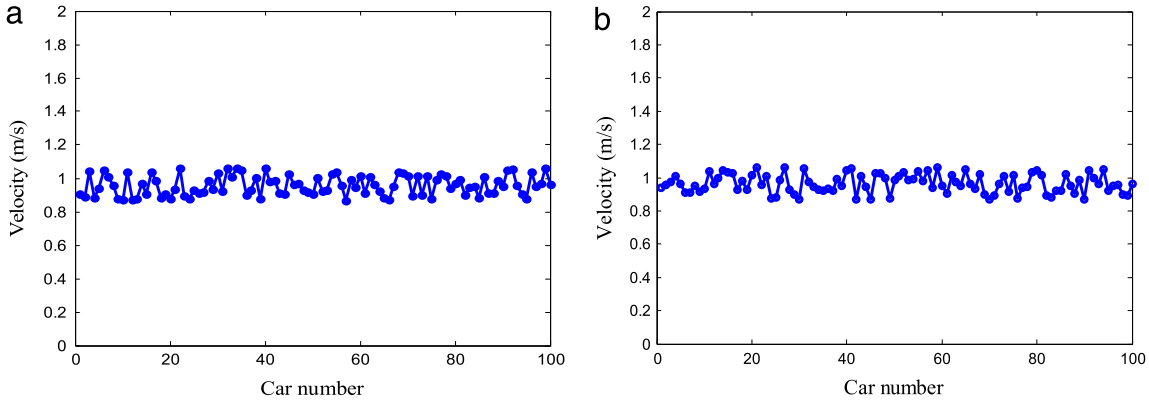

Fig. 11. Velocity profile of vehicular traffic flow ($t = 100$ s): (a) Feedback control strategy; (b) SMC strategy.

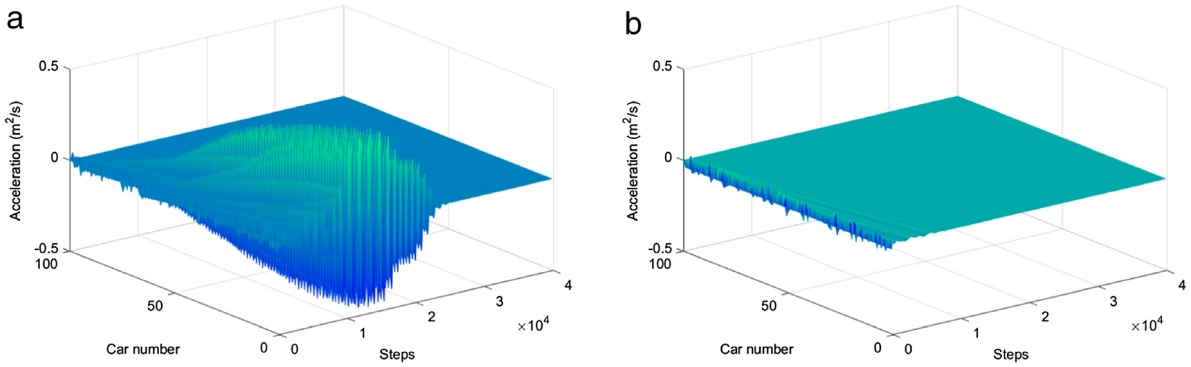

Fig. 12. Acceleration profile of vehicular traffic flow ($t = 400$ s): (a) Feedback control strategy; (b) SMC strategy.

5. Conclusions

This study analyzes the smoothness and stability aspects of vehicular traffic flow with and without the use of control strategies. It proposes a sliding mode controller of vehicular traffic flow based on the FVD model. In particular, the study seeks to analyze the performance of the proposed SMC strategy in terms of smoothness and stability of vehicular traffic flow, and whether it can enable such smoothness and stability more quickly compared with the commonly-used feedback control strategy. The stability of the proposed controller is guaranteed using the Lyapunov technique. Simulation-based numerical experiments are used to verify the effectiveness of the proposed controller. Compared with the feedback control and no control strategies, the distribution smoothness and stability associated with the space headway, velocity and acceleration profiles of vehicular traffic flow are improved significantly from a computational efficiency standpoint.

Simulation results show that traffic fluctuation can be stabilized using the proposed sliding mode controller in a more responsive manner. It highlights the need to develop traffic management strategies to regularize vehicular traffic flow through appropriate control strategies that can enable the traffic to flow more homogeneously.

Acknowledgments

The authors would like to acknowledge the support from the National Natural Science Foundation of China (Grant No. 61304197), the Scientific and Technological Talents of Chongqing (Grant No. cstc2014kjrc-qnrc30002), the Key Project of Application and Development of Chongqing (Grant No. cstc2014yykfB40001), "151" Science and Technology Major Project of Chongqing—General Design and Innovative Capability of Full Information based Traffic Guidance and Control System (Grant No. cstc2013jcsf-zdzxqqX0003), the Doctoral Start-up Funds of Chongqing University of Posts and Telecommunications, China (Grant No. A2012-26), National Key Research and Development Program, (Grant No. SQ2016ZY02002100) and the U.S. Department of Transportation through the NEXTRANS Center, the USDOT Region 5 University Transportation Center.

References

[1] R. Wilson, J. Ward, Car-following models: fifty years of linear stability analysis–a mathematical perspective, Transp. Plan. Technol. 34 (1) (2011) 3–18.
[2] Y. Li, D. Sun, Microscopic car-following model for the traffic flow: the state of the art, J. Control Theory Appl. 10 (2) (2012) 133–143.
[3] M. Bando, K. Hasebe, A. Nakayama, A. Shibata, Y. Sugiyama, Dynamical model of traffic congestion and numerical simulation, Phys. Rev. E I (51) (1995) 1035–1042.
[4] D. Helbing, B. Tilch, Generalized force model of traffic dynamics, Phys. Rev. E 58 (1998) 133–138.
[5] R. Jiang, Q. Wu, Z. Zhu, Full velocity difference model for a car-following theory, Phys. Rev. E 64 (1) (2001) 017101–017105.
[6] D. Sun, Y. Li, C. Tian, Car-following model based on the information of multiple ahead & velocity difference, Syst. Eng.-Theory Pract. 30 (7) (2010) 1326–1332.
[7] X. Zhao, Z. Gao, A new car-following model: full velocity and acceleration difference model, Eur. Phys. J. B 47 (2005) 145–150.
[8] T. Wang, Z. Gao, X. Zhao, Multiple velocity difference model and its stability analysis, Act. Phys. Sinica. 55 (2006) 634–638.
[9] Y. Li, D. Sun, W. Liu, M. Zhang, M. Zhao, X. Liao, L. Tang, Modeling and simulation for microscopic traffic flow based on multiple headway, velocity and acceleration difference, Nonlinear Dynam. 66 (1–2) (2011) 15–28.
[10] Y. Li, H. Zhu, M. Cen, Y. Li, R. Li, D. Sun, On the stability analysis of microscopic traffic car-following model: a case study, Nonlinear Dynam. 74 (1–2) (2013) 335–343.
[11] T. Tang, W. Shi, H. Shang, Y. Wang, A new car-following model with consideration of inter-vehicle communication, Nonlinear Dynam. 76 (4) (2014) 2017–2023.
[12] T. Tang, J. Li, H. Huang, X. Yang, A car-following model with real-time road conditions and numerical tests, Measurement 48 (2014) 63–76.
[13] T. Tang, J. Li, S. Yang, H. Shang, Effects of on-ramp on the fuel consumption of the vehicles on the main road under car-following model, Physica A 419 (2015) 293–300.
[14] T. Tang, J. He, S. Yang, H. Shang, A car-following model accounting for the driver's attribution, Physica A 413 (2014) 583–591.
[15] T. Tang, H. Huang, H. Shang, Influences of the driver's bounded rationality on micro driving behavior, fuel consumption and emissions, Transp. Res. D 41 (2015) 423–432.
[16] T. Tang, Y. Wang, X. Yang, Y. Wu, A new car-following model accounting for varying road condition, Nonlinear Dynam. 70 (2012) 1397–1405.
[17] T. Tang, L. Chen, S. Yang, H. Shang, An extended car-following model with consideration of the electric vehicle's driving range, Physica A 430 (2015) 148–155.
[18] S. Yu, Z. Shi, An improved car-following model considering headway changes with memory, Physica A 421 (2015) 1–14.
[19] Y. Li, K. Li, T. Zheng, X. Hu, H. Feng, Y. Li, Evaluating the performance of vehicular platoon control under different network topologies of initial states., Physica A 450 (2016) 359–368.
[20] Y. Li, L. Zhang, S. Peeta, X. He, T. Zheng, Y. Li, A car-following model considering the effect of electronic throttle opening angle under connected environment, Nonlinear Dynam. (2016) http://dx.doi.org/10.1007/s11071-016-2817-y.
[21] Y. Li, L. Zhang, B. Zhang, T. Zheng, H. Feng, Y. Li, Non-lane-discipline-based car-following model considering the effect of visual angle, Nonlinear Dynam. (2016) http://dx.doi.org/10.1007/s11071-016-2803-4.
[22] S. Jin, D. Wang, P. Tao, P. Li, Non-lane-based full velocity difference car following model, Physica A 389 (21) (2010) 4654–4662.
[23] Y. Li, L. Zhang, S. Peeta, H. Pan, T. Zheng, Y. Li, X. He, Non-lane-discipline-based car-following model considering the effects of two-sided lateral gaps, Nonlinear Dynam. 80 (1–2) (2015) 227–238.
[24] Y. Li, L. Zhang, H. Zheng, X. He, S. Peeta, T. Zheng, Y. Li, Evaluating the energy consumption of electric vehicles based on car-following model under non-lane discipline, Nonlinear Dynam. 82 (1) (2015) 629–641.
[25] K. Konishi, H. Kokame, K. Hirata, Coupled map car-following model and its delayed-feedback control, Phys. Rev. E 60 (4) (1999) 4000–4007.
[26] K. Konishi, H. Kokame, K. Hirata, Decentralized delayed-feedback control of an optimal velocity traffic model, Eur. Phys. J. B 15 (2000) 715–722.
[27] X. Zhao, Z. Gao, Controlling traffic jams by a feedback signal, Eur. Phys. J. B 43 (2005) 565–572.
[28] Y. Li, D. Sun, W. Liu, Feedback control of traffic jam based on the full velocity difference car-following model, J. Inf. Comput. Sci. 3 (2012) 719–730.
[29] Y. Li, L. Zhang, T. Zheng, Y. Li, Lattice hydrodynamic model based delay feedback control of vehicular traffic flow considering the effects of density change rate difference, Commun. Nonlinear Sci. Numer. Simul. 29 (1–3) (2015) 224–232.
[30] Y. Li, B. Yang, T. Zheng, Y. Li, M. Cui, S. Peeta, Extended-state-observer-based double-loop integral sliding-mode control of electronic throttle valve, IEEE Trans. Intell. Transp. Syst. 16 (5) (2015) 2501–2510.
[31] X. Zhang, Y. Fang, N. Sun, Minimum-time trajectory planning for underactuated overhead crane systems with state and control constraints, IEEE Trans. Ind. Electron. 61 (12) (2014) 6915–6925.
[32] N. Sun, Y. Fang, H. Chen, A new antiswing control method for underactuated cranes with unmodeled uncertainties: Theoretical design and hardware experiments, IEEE Trans. Ind. Electron. 62 (1) (2015) 453–465.
[33] Y. Li, B. Yang, T. Zheng, Y. Li, Extended state observer based adaptive back-stepping sliding mode control of electronic throttle in transportation cyber-physical systems, Math. Probl. Eng. 2015 (2015).
[34] S. Bhat, D. Bernstein, Finite-time stability of continuous autonomous systems, SIAM J. Control Optim. 38 (3) (2000) 751–766.
[35] J. Kwon, D. Chwa, Adaptive bidirectional platoon control using a coupled sliding mode control method, IEEE Trans. Intell. Transp. Syst. 15 (5) (2014) 2040–2048.
[36] H. Pan, W. Sun, H. Gao, J. Yu, Finite-Time stabilization for vehicle active suspension systems with hard constraints, IEEE Trans. Intell. Transp. Syst. 16 (5) (2015) 2663–2672.